MINERAL SCALING IN GEOTHERMAL TWO-PHASE PIPELINES

Jansell Jamero* and Sadiq J. Zarrouk

Department of Engineering Science, The University of Auckland, Private Bag 92019, Auckland, New Zealand

*jjam895@aucklanduni.ac.nz

Keywords: *Two-phase, Mineral scaling, Geothermal pipeline, ESEM-EDS, XRD.*

ABSTRACT

Mineral scaling is a common problem in geothermal power facilities. This scale deposition is usually caused by changes in the geothermal fluid temperature or composition. Precipitation of these minerals can limit fluid flow within the steam field equipment, reducing plant efficiency and increasing maintenance costs.

A layer of scaling is commonly found in most parts of the geothermal power production facilities. However, significant amounts of deposited mineral scales (mainly silica) are usually observed in the pipelines and vessels that handle super-saturated brines.

This work focuses on a less common scaling in geothermal two-phase pipelines, when fluids are usually high in temperature and under-saturated with respect to amorphous silica. This is mainly caused by fluid mixing at the two-phase pipelines, when several wells share the same pipeline header to transport the fluid to the downstream facility.

Two case studies are discussed in this work reporting mineral scaling due to the mixing of incompatible geothermal fluids within two-phase headers.

The first case investigates silica deposition caused by the mixing of a steam-dominated well fluid with fluid from two water-dominated wells. The scale deposition is caused by the small amount of brine entrained in the steam-dominated well fluid which reacts upon mixing with the fluid from the other water-dominated wells, causing massive localised scaling at the mixing points. The second case investigates iron mineral and silica deposition caused by the mixing of a low-pH, high-silica fluid with neutral-pH fluid.

Header blockage result in the increase in well head pressures causing production from some wells to collapse, at the same time decreasing the flow of geothermal fluids to the separators. The scaling requires regular cleaning to return the pipelines to full flow capacity. Recommended engineering solutions are given for both cases, for possible site implementation.

1. INTRODUCTION

1.1 Mineral Scaling in Geothermal Environment

Geothermal energy is simply the heat from the earth. To utilise this heat, a carrier deep groundwater/fluid is needed to transfer this energy to the surface for utilization (Barbier, 2002). The underground reservoirs that host this fluid can be accessed by drilling wells from the surface down to a few kilometres (Gupta, et al., 2006). The extracted hot fluid is then conducted through pipelines where it will be utilised to generate electricity. Electricity generation is commonly done by separating the steam component of the fluid and running it through a turbine. The turbines are connected to electric generators, which turns the turbines' mechanical energy into electrical energy.

The chemistry of the geothermal fluid is dependent on the type of geothermal reservoir; hence the composition of the geothermal fluid varies from one geothermal system to the other and it can also vary within the same geothermal system. These differences are due to variations in temperature, gas content, heat source, rock type, rock permeability, age of the hydrothermal system and fluid source (Barbier, 2002).

One of the common challenges facing geothermal development is mineral scale deposition. When the highly mineralised geothermal fluids are extracted, they are subjected to changes in temperature and pressure. These changes can lead to the deposition of the dissolved minerals (solids), which cause problems to the pipelines and power plant equipment.

1.2 Scaling in Geothermal Surface Facility

Mineral deposition can occur at any point within the geothermal surface facility. Following the path of the fluid upon reaching the surface, changes in temperature may lead to thermodynamic reactions that can cause scaling (fouling). Changes (drops) in pressure can also lead to the release of dissolved gases from the fluid, changing its component concentrations which can lead to more scaling. When the fluid is travelling along pipelines to the different vessels, kinetic scaling reactions may take place and deposit minerals along the way. Figure 1, below, illustrates the common locations for the different mineral deposits encountered in a typical single flash geothermal power production system (Tassew, 2001).

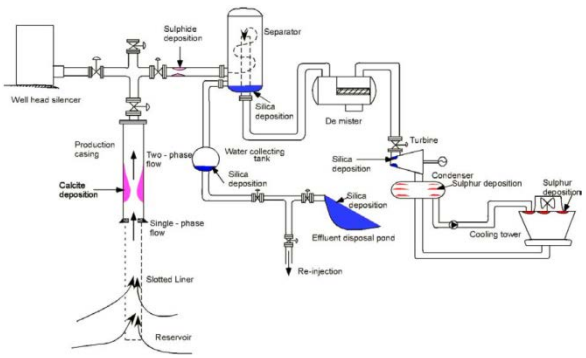

Figure 1: Flow diagram of a geothermal system with common locations of different mineral scales (from Tassew, 2001).

In general, surface facility scaling will lead to the loss of capacity for the pipelines, vessels and equipment within the process. This, in turn, will decrease the efficiency of the geothermal plant (Phillips, et al., 1979). Furthermore, if the scaling is extensive, a shutdown may be needed to clear the lines and equipment and enable running the facility to full capacity (Villaseñor, et al., 2011). When scaling is

experienced repeatedly, it increases maintenance cost and reduces the plant availability.

Deposition can also occur within the vessels holding the fluid. Geothermal steam-water separators and holding tanks are expected to have some scaling due to their ability to hold large volumes of fluids. Turbines can also experience scaling when the steam used has some carry-over brine (rich in minerals). In binary power plants and direct use applications of geothermal energy equipment, mineral scaling is commonly found in the heat exchanger, as seen at the Soultz-sous-Forêts EGS site (Scheiber, et al., 2015). Heat exchanger tube fouling commonly occurs because of the significant drop in temperature along the length of the tubes. It increases the thermal resistance of the walls and decreases the available pipe diameter, both of which are detrimental to the efficient utilization (Zarrouk, et al., 2014).

1.3 Scaling Treatment Methods

To utilise the surface facilities, scale deposition has to be mitigated or controlled. However, scaling treatment methods are dependent on the site conditions and chemistry of the geothermal fluid within the system. The success and feasibility of the treatment is usually site specific (Formento, et al., 2012).

A number of methods have been investigated for the prevention and mitigation of mineral scaling in geothermal facilities. The usual method of scale removal is through mechanical scraping. Typically, acid is added before scraping and then it is washed with water to remove the products (Phillips, et al., 1979). However, this is mostly for scale deposits that have already formed. This is usually a maintenance issue and is scheduled on as needed bases.

For scale control, Phillips, et al. (1979) categorised the treatment methods into inhibitors (which retard the growth of scale), alterants (which change the chemistry of the geothermal fluid) and coagulants/flocculants (which help remove precipitates or suspended substances from the solution). Selecting the optimal treatment method is established by combining the need to prevent scaling and to avoid affecting the temperature and flow rate of the geothermal fluid.

Engineering design can also be used which will collect the deposits within an area where they can be easily removed and cleaned out, or through the use of instruments that keep the deposits in suspension (van Rosmalen, 1983). By determining the chemical composition of the geothermal waters before production, the possible types of scale and extent of scaling can be predicted and may help in determining what methods to implement to resolve the problem. Further comprehension of the tested inhibition methods is also needed to determine their appropriate application within the system.

2. SCALE EVALUATION METHODOLOGY

For the two case studies (pad A and pad B) that will be presented, representative scale samples were taken at different locations along the two-phase headers lengths. The samples were stored in plastic vials and labelled based on their location along the two-phase pipeline. These samples were then prepared, photographed and analysed for their elemental and mineral components.

An FEI Quanta 200 F Environmental Scanning Electron Microscope (ESEM) was used to analyse the scale samples. It is equipped with a Field Emission Gun (FEG) and has an Electron Backscatter Diffraction (EBSD) Detector attachment. Before analysis, the samples were cut into small pieces and mounted on a sample holder with a 1 cm diameter face (Figures 2 and 3). These took 24 hours to dry before being coated with a platinum conductive coating using a Quorum Q150RS Sputter Coater. The samples were then loaded into the ESEM for high magnification photos using a Large Field Detector (LFD). Energy Dispersive X-Ray Spectroscopy (EDS) can also be carried out by the same scanner. Use of the Solid State Detector (SSD) of the EBSD enabled elemental analysis of the surface of the samples.

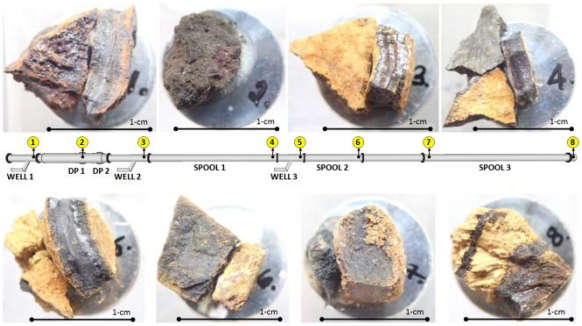

Figure 2: ESEM-EDS samples and their corresponding locations on the pad A two-phase header.

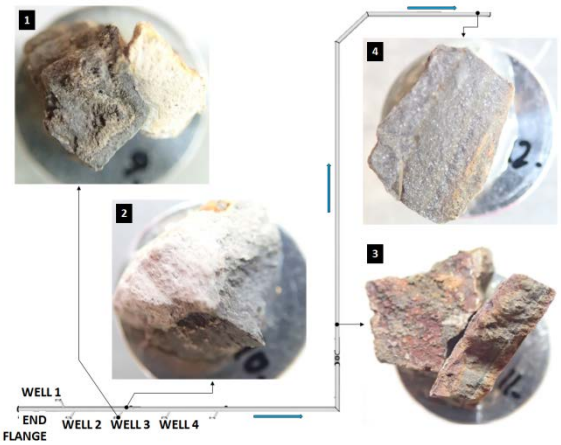

Figure 3: ESEM-EDS samples and their corresponding locations on the pad B two-phase header.

For the identification of the mineral components of the samples, a Panalytical Empyrean™ X-Ray Diffractometer (XRD) was used. The samples were ground down to a fine powder before analysis. The samples were then loaded all at once, with the instrument running the samples one at a time. The XRD produces an angle versus intensity graph which can be run through library software MATCH!© to determine which intensity peak belongs to which mineral.

3. CASE STUDY 1: MIXING OF A STEAM-DOMINATED FLUID WITH TWO-PHASE FLUIDS IN A COMMON HEADER

The Upper Mahiao sector of the Leyte geothermal system, the Philippines reported significant scaling at pad A. The pad currently has three production wells drilled. Well 1 is a high enthalpy, steam-dominated well. Its liquid flow rate decreased from a maximum of 2.6 kg/s to zero since

October of 2011. Wells 2 and 3 are both liquid-dominated wells with slightly below neutral pH of 5.79 and 6.23 respectively. All three wells mix in a single two-phase header before the fluid is sent to the separation station. The latest flow rate measurement and complete chemistry for the three wells are shown in Tables 1 to 3.

Table 1: Flow rates for pad A wells on December 2014.

Well	MPa g	kJ/kg	kg/s		°C
	Well head Pressure	**Measured Enthalpy**	**Steam Flow**	**Water Flow**	**Down-hole Temp**
1	1.55	2790	18.5	0	311
2	1.78	1645	7.1	9.5	298
3	1.6	1667	11.31	14.55	241

Table 2: Water chemistry for pad A wells on December 2014.

Well	pH	mg/kg					
		Cl	**SO_4**	**CO_2**	**H_2S**	**SiO_2**	**Ca**
1	-	-	-	-	-	-	-
2	5.46	10417	19	31.3	0	869	155
3	6.3	4364	32.7	49.7	0	555	66.5

continuation of previous table…

mg/kg							
Mg	**Fe**	**K**	**Na**	**NH_3**	**B**	**Li**	**HCO_3**
-	-	-	-	-	-	-	-
0.16	0.5	1422	5742	3.48	223	27	15.1
0.1	0.33	406	2596	3.54	117	9.7	39.5

Table 3: Gas chemistry for pad A wells (December 2014.

Well	mmoles/100 moles steam						
	CH4	**CO_2**	**H_2**	**H_2S**	**N_2**	**NH_3**	**Ar**
1	1.23	479	4.809	46.8	47.95	-	-
2	1.84	731	5.442	58.4	72.73	1.72	-
3	3.02	593	1.844	24.6	15.92	1.61	0.22

The Cl-SO4-HCO3 ternary diagram (Figure 4) shows both wells 2 and 3 as neutral-pH wells with high chloride concentration. Well 1 is not included in the diagram because it has no measurable brine flow.

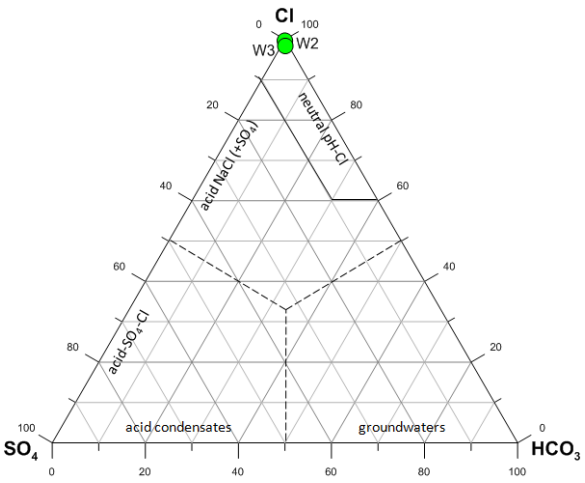

Figure 4: Cl-SO4-HCO3 ternary diagram for pad A wells.

On the other hand, the Na-K-Mg ternary diagram (Figure 5) shows that both wells are from a mature reservoir where its fluids have already equilibrated with the surrounding rocks and minerals. The derived temperatures from Figure 5, for each well, is higher than the measured down-hole temperature (Table 1); but it shows that well 2 has a higher temperature than well 3 following the same trend as the down-hole temperatures in Table 1.

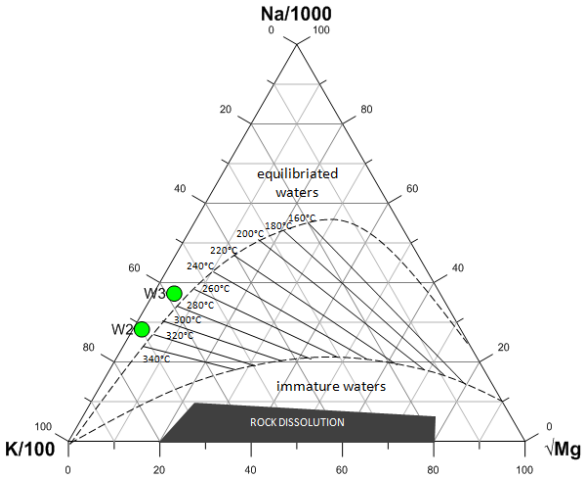

Figure 5: Na-K-Mg ternary diagram for pad A wells.

3.1 Background on the January 2015 Inspection

Well flow tests have shown that the water component of well 1 has been zero since October of 2011. However, the presence of scale deposits at the well 1 stub-in point showed that some brine was still present. To remove this water component and prevent it from reacting with the other well fluids, two 30" (76.2 cm) oversized drain pots (ODP) were installed after the well 1 stub-in (Figure 6). These pots were regularly drained of fluid and opened annually to remove accumulated solids that were deposited or transported by well 1. Solid samples were taken after 3 months and petrology analysis showed that they were made up of mostly corrosion products (75-80%) of hematised magnetite, amorphous silica (15%) enclosed by the corrosion products and some entrained rock materials (5-10%) made up of mostly calcite and rare feldspar (Ramos, 2013).

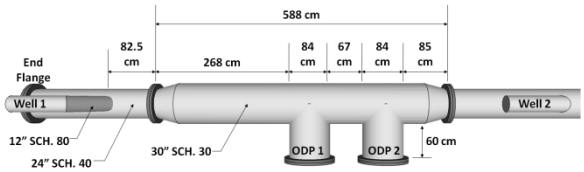

Figure 6: Side view of the oversized drain pots (ODP) installed at pad A two-phase header.

The ODPs installed were inspected again on January 2014 due to complications in draining of the accumulated fluid. Due to the solids entrained in the steam-dominated fluid of well 1, the draining system for the ODPs tended to get blocked. Leaking of the drain pipes also occurred which led to replacements and re-orientation from the bottom drain valve to the side drain valve. The configuration of the two-phase header in pad A is shown in Figure 7.

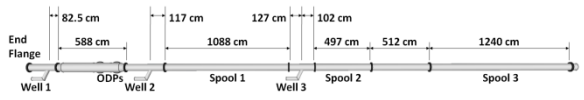

Figure 7: Top view of the pad A two-phase header as of June 2013.

We will focus on the inspection made in January 2015. Prior to the two-phase header shutdown, well 1 had continued to produce a non-measurable water component while wells 2 and 3 are water-dominated (Table 1). The well 2 chemistry was slightly more acidic than well 3 and well 2 also had higher sodium and chloride concentrations than well 3 (Table 2). Gas chemistry, on the other hand, showed a few minor differences between the three wells (Table 3).

Historical WHP trending for all three wells prior to the inspection is shown in Figure 8. Figure 8 shows that the WHP for wells 1 and 2 increased in the second half of 2014. This usually signifies scaling at the two-phase header (Figure 7). Well 3 WHP, on the other hand, appears to be stable below 1.5 MPag in the second half of 2014.

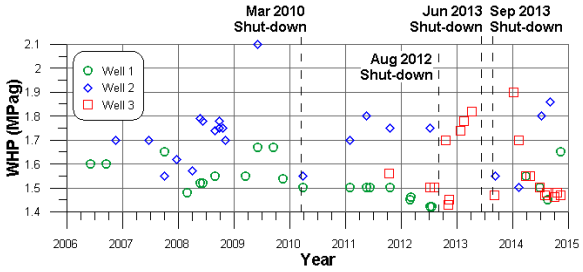

Figure 8: Well head pressures of pad A wells 1, 2, and 3, since cut-in until the January 2015 two-phase header shutdown.

The total suspended solids (TSS) of well 1 (Figure 9) show that branch-line samples were mostly below 10 mg/kg in 2013; however, samples taken from the ODPs have TSS values of over 1000 mg/kg after some time. These can be associated with the accumulation of solids at the drain pots which likely increases the TSS concentration of the collected fluid.

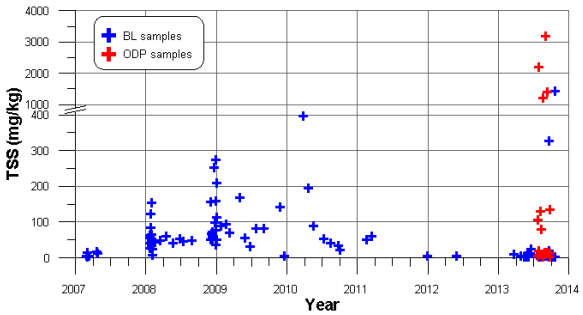

Figure 9: Total suspended solids (TSS) concentration of pad A well 1, with samples taken from the branch-line (BL) and the oversized drain pots.

Documentation of the pad A two-phase header inspection is shown in Figure 10. Figure 10 shows a 12 cm thick solid scale accumulation at the end flange, before the stub-in point of well 1 (Figure 10A). The depositions taper off toward the well 1 stub-in, though scaling is seen from the top to the bottom of the pipe. As expected, the drain pots downstream of well 1 were full of transported and deposited solids.

Figure 10 also shows that upon mixing the fluids of well 1 with well 2, the depositions increased to a maximum 36 cm thick scale at the bottom of the pipe (Figure 10B). The pipe diameter is reduced to almost 25% due to scaling on the pipe walls. However, the scales also taper off to about a maximum of 25 cm at the bottom, right before the mixing point of well 3 (Figure 10C). The addition of well 3 fluids reduced the pipe diameter to about 10%, as seen in Figure 10D. From there, the depositions gradually becomes thinner, to around 18 cm (Figure 10E) until they reach a 13 cm thick deposition from the bottom (20 m from the well 3 mixing point) (Figure 10F).

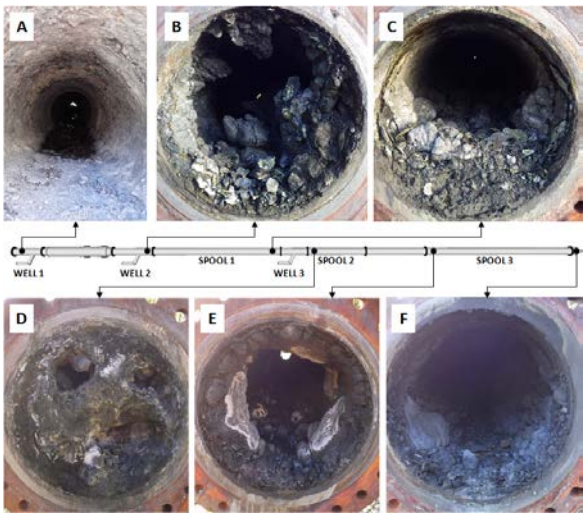

Figure 10: Scaling in pad A two-phase mixing header documented on January 2015.

3.2 Results

Pad A two-phase header has no measured temperature or pressure. At the same time collecting fluid samples was not possible due to the scaling. Since well 1 WHP was measured at 1.55 MPag (Table 1) and the well branch-line is not very long, a pressure of 1.5 MPaa (and temperature of 198°C) can be assumed for the two-phase header.

Calculated silica saturation index (SSI) for wells 2 and 3 are 0.96 and 0.60, respectively. These values show that the produced fluids are not supersaturated with silica, which is proven in the lack of silica deposits within the individual branch-lines. However, the documentation shows that mixing of the well fluids induces the formation of massive deposits of silica scale. To determine the occurrence of flashing at the estimated header pressure of 1.5MPaa, the calculations show no brine flashing from wells 2 and 3, but show a calculated 0.0095 kg/s brine flow from well 1. This small value of water flow could not be captured or measured physically.

The small brine flow from well 1 could hold enough supersaturated minerals to initiate the deposition of scale upon mixing with the fluid of wells 2 and 3. Also, documented erosion within the branch-line of well 1 (Figure 11) could contribute to the iron content of the two-phase header's fluids. Figure 11 shows evident erosion within the branch-line of well 1. Also, there was some deposition within the pipe walls which supports the theory that the small brine from well 1 does have supersaturated dissolved minerals that can deposit. However, with the small amount of brine, scaling in the well 1 branch-line is manageable.

Figure 11: Well 1 branch-line sweep bend inspected on June 2013, showing significant erosion damage.

Mixing of the small amount of supersaturated brine from well 1 with the brine of wells 2 and 3 was enough to cause the mineral deposition at the two-phase header.

To verify if a trend can be determined from the XRD results, the weight percentages generated from samples 1 to 8 (Figure 2) were placed in a graph relative to their location, as seen in Figure 12.

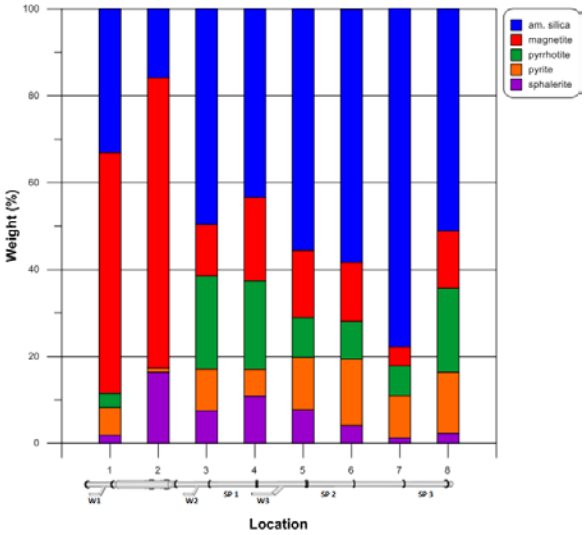

Figure 12: XRD mineral scale distribution of each sample based on its location in the pad A two-phase header.

Figure 12 show that locations 1 and 2 produce high magnetite followed by silica. Since only fluid from well 1 is present in these locations, while silica is present in smaller amount in the brine but enough to deposit silica along the walls. It is most likely that the iron forming the magnetite is from the branch-line pipe walls which were eroded (Figure 11), as the steam-dominated fluid passed through the line.

Mixing of well 2 fluids at location 3 increased the weight of silica in proportion to the rest of the scale minerals. This was due to the addition of 9.5 kg/s of brine fluid (Table 1) with 869 mg/kg of silica (Table 3 2). With well 2 SSI already at 0.96, introduction of more silica from the supersaturated brine of well 1 will increase the SSI of the mixed fluid. The presence of suspended iron solids from well 1 may have also served as nuclei for silica deposition enabling faster formation and deposition within this mixing area. Comparing the silica weight percentage from locations 3 and 4, we notice a slowing of silica deposition. This is due to the almost instantaneous deposition of silica within location 3, from the mixing of wells 1 and 2. This rapid formation of silica enabled most of the dissolved mineral to deposit at that location leaving the silica formation in location 4 in decline in comparison.

Silica deposition increased again in location 5 due to the mixing of well 3 fluids. Well 3 introduce 555 mg/kg of silica (Table 2) to the header fluids. The increasing weight percentage of silica from locations 5 to 7 indicates that the scale formation after well 3 mixing was due to the gradual forming of silica scale. This scale gradually formed and deposited along the pipe, increasing the percentage of silica on the total weight of the mineral deposits. By location 8, silica deposition starts to decline indicating that most of the silica dissolved within the fluid was already deposited upstream of that location.

Iron deposits are observed in all points and compose about 50% by weight of the scale despite the low brine iron content of wells 2 and 3 (Table 2). The iron from the eroded pipeline walls is therefore responsible for the presence of the iron deposits within the header. The presence of zinc in the ESEM data also explains the occurrence of sphalerite in the scale samples.

3.3 Recommended Solutions

Mitigation of the two-phase header mineral scaling is dependent on the handling of the small flow rate of brine from well 1. Mixing of only wells 2 and 3 may still result in mineral scaling; however, it is expected to be gradual and manageable since SSI values for both fluids are below 1.0 (saturation). Also, since no flashing occurs within the header pipeline, there is no expected increase in SSI in fluid of either wells.

3.3.1 Extension of Branch-Line

The small amount of brine from well 1 travels through the pipe in two ways: (1) as liquid droplets dispersed within the steam flow, and (2) as liquid flowing along the pipe walls. To remove the brine moving with the steam (point 1), we can follow the calculations by Arifien, et al. (2015).

For a certain steam velocity, a horizontal pipeline length can be calculated to enable liquid droplets to fall to the bottom of the pipe. Arifien, et al. (2015) used droplet sizes ranging from 5 to 500 μm. To eliminate the need to define the pipe diameter, the assumption was made that the droplets were distributed uniformly within the pipe cross-section. Then, if the fraction of droplets which existed within a distance from the bottom of the pipe were evaluated (Figure 13), circle geometry could then be used to determine the relation between h/D and Ao/A. Comparing h/D and Ao/A values shows that for $h \approx 0.3D$, the Ao/A is 25%; and for a 75% Ao/A, h should be $\approx 0.7D$.

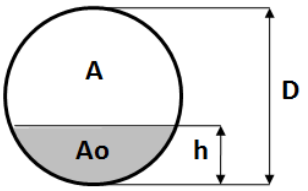

Figure 13: Partial and full cross-sectional area of pipe (from Arifien, et al., 2015).

The calculations made by Arifien, et al. (2015) show that for a steam velocity of 36.4 m/s, a brine droplet diameter of 100 μm and larger is needed to enable 75% of the pipe droplets to reach the bottom after 100 m of pipeline. For droplet sizes smaller than that, long pipes are needed to enable gravity settling to the bottom of the pipe.

Comparing this with our steam velocity for the well 1 branch-line, which is calculated at 37.18 m/s, we would need longer pipe runs than those calculated by Arifien, et al. (2015) since horizontal pipe length is directly proportional to the steam velocity. Given that the existing branch-lines are less than 100 m in length, there is not enough pipe distance for the smaller brine droplets in well 1 to fall to the bottom of the branch-line. Extending the pipe length to accommodate the calculated length needed would be impractical.

3.3.2 Modification of Existing ODPs with Baffle Plates

The currently installed ODPs, after the introduction of well 1 into the header is a step in the right direction to capture the brine droplets from the steam flow of well 1. The expansion of the pipe from the 12" (30.48 cm) branch-line slowed down the steam flow from 37.18 m/s to 5.82 m/s by the time it reached the 30" (76.2 cm) oversized pipe header. However, given the short lengths of the 24" (60.96 cm) header and 30" (76.2 cm) oversized pipe, we do not expect most of the brine droplets to drop to the bottom and into the ODPs.

We can improve the current design by incorporating a flow guide on the walls before the ODPs, as seen in Figure 14. This was recommended by Arifien, et al. (2015) to improve the performance of the scrubbing line. The flow guides on the wall are diagonal to lead the brine flow along the walls towards the drain pot at the bottom. A baffle could also be added in the drain pot itself to improve their efficiency. However, further examination and appropriate design calculations are needed to prevent possible re-entrainment of brine droplets back into the steam flow.

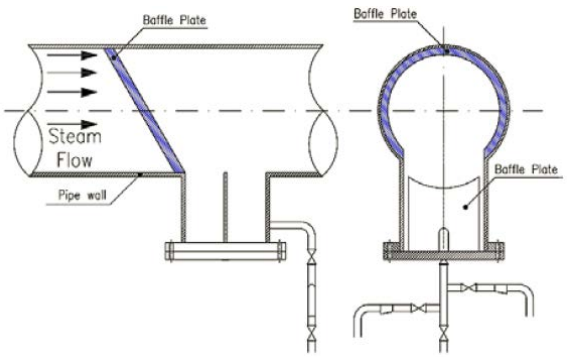

Figure 14: Proposed baffle installation to improve line scrubbing (from Arifien, et. al., 2015).

3.3.3 Modification of Existing ODPs with BLISS Separator

The design of the existing ODPs assumes that the brine particles will fall to the bottom of the pipe due to gravity. This, however, does not consider the brine that is entrained in the steam and travelling along the center of the pipeline. To target these brine particles, the BLISS concept could be utilised. The Boundary Layer Inline Separator Scrubber, or BLISS, is a type of geothermal steam purifier which uses the pipeline as a part of the separator (Jung, et al., 2000).

Based on the BLISS design, shown in Figure 15, the wet stean goes through a spin generator which produces an annular liquid profile, keeping the liquid against the walls by high centrifugal force. As the fluids enter the perforated liner, the liquid is then squeezed through the holes as it passes. The separated liquid is then collected at the bottom of the shell through a drain pot (Figure 15).

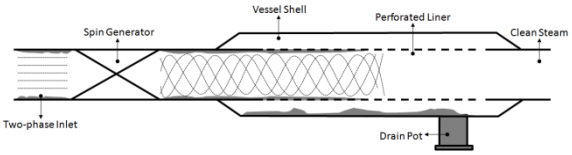

Figure 15: Cross-sectional view of the BLISS (modified after Jung, et al., 2000).

With the existing ODPs installed in the pad A two-phase header, only the spin generator and perforated liner need to be installed to implement the BLISS design. Jung, et al. (2000) also state that the BLISS can be used for separation of entrained solids, which is also an issue for well 1.

3.3.4 Installation of an In-Line Vortex Separator

A vortex separator could also be installed along the branch-line of well 1 to separate the entrained brine particles before it mixes with the fluids inside the header. A vortex separator is a truncated cone laid horizontally with fixed helicoid vanes near the inlet which would facilitate the formation of a vortex (Figure 16). This vortex would exert a centrifugal force on the water droplets pushing them to the separator walls where it can be collected (Lee, 1995).

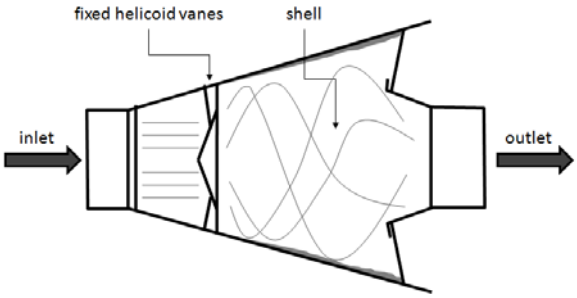

Figure 16: Cross-sectional view of a vortex separator (modified after Lee, 1995).

This method of brine separation is similar to the BLISS separator discussed previously; however, this should be installed in the well 1 branch-line rather than the pad A two-phase header. Installation of the vortex separator plus the modification of the existing ODPs could possibly remove all the entrained brine from well 1.

3.3.5 Installation of a Wet Scrubber

Wet scrubbing can also be used for brine droplet removal from well 1 steam. Hjartarson, et al. (2012) defined wet scrubbing as the traditional method for the removal of unwanted volatile liquid or entrained brine from superheated geothermal steam. Since well 1 is predominantly steam, the spraying of water into the system will enable the finer brine droplets to agglomerate with the larger water droplets (Arifien, et al., 2015). The larger and heavier water droplets will then drop to the bottom of the pipe and accumulate in the ODPs. However, there is a loss of heat and decline in the energy recovered from the well associated with wet scrubbing. Also, the addition of water

will need an efficient draining of the ODPs to prevent liquid accumulation and re-introduction of the removed brine into the two-phase header system.

3.3.6 Throttling of Steam-dominated Well 1

Since well 1 and its entrained brine is the cause of the mineral scaling, throttling of the well could lessen the deposition within the two-phase header. There will also be less steam flowing through the over-sized pipeline slowing the velocity further and enabling more brine particles to drop to the ODPs. Throttling of the well will also lessen the amount of erosion products carried to header. This will lessen the blockage of the ODP drainage system and also prevent the addition of iron to the header fluids. The decrease in steam production, however, may not be economically comparable to the maintenance costs of pipe cleaning.

3.3.7 Increase Branch-Line Diameter

Another way is to enlarge the branch-line of well 1. Enlargement of the pipe will decrease the steam velocity and lessen the erosion effects; however, this entails replacement of existing pipelines and connections. Unless well 1 increases its production significantly, this will not be an economical solution to the erosion issue.

4. CASE STUDY 2: MIXING OF A LOW-PH, HIGH-SILICA FLUID WITH NEAR-NEUTRAL PH TWO-PHASE FLUIDS

Pad B is located in the Mahanagdong-B sector of the Leyte geothermal field in the Philippines. The pad is located on an isolated portion of the field and is a few kilometers away from the separation station. It currently has four production wells contributing to the system through a common 42" (1.06 m) two-phase header (Figure 17).

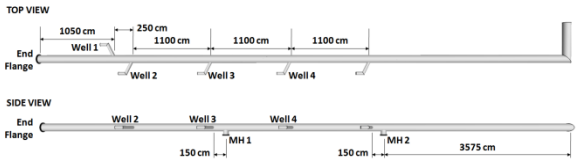

Figure 17: Top and side views of pad B two-phase header as of January 2015.

The wells were introduced to the system in this order: (a) well 2 on July 1, 2010; (b) well 4 on August 10, 2010; (c) well 3 on May 8, 2011; and (d) well 1 on May 31, 2014. Fluids from wells 1 and 4 are slightly acidic, with a pH of 5.49 and 5.59, respectively. On the other hand, the low-pH fluids were contributed by well 2 (pH = 3.46) and well 3 (pH = 3.54). Well 3 is also the main contributor of silica to the system, with concentrations fluctuating around 1000 mg/kg. The flow rates and liquid and gas chemistry of the four wells are listed in Tables 4 to 6.

Table 4: Flow rates for pad B wells on January 2015.

Well	MPag	kJ/kg	kg/s		
	Well head Pressure	**Enthalpy**	**Total Mass Flow**	**Water Flow**	**Steam Flow**
1	1.25	2358	39.7	8.5	31.2
2	0.95	1894	7.5	3.4	4.2
3	1.2	1538	74.2	46.6	27.7
4	1.13	1989	12.4	5.0	7.5

Table 5: Water chemistry for pad B wells on January 2015.

Well	pH	mg/kg						
		Li	**Na**	**K**	**Ca**	**Mg**	**Fe**	**Cl**
1	5.49	5.59	1681	452	38	-	0.21	3137
2	3.46	7.15	2978	373	17.2	47.8	40.3	4398
3	3.54	9.99	2841	767	139	3.6	19.8	5461
4	5.59	1.84	1296	100	2.15	3.79	0.4	1118

continuation of previous table…

mg/kg							
SO_4	**HCO_3**	**B**	**NH_3**	**SiO_2**	**H_2S**	**CO_2**	**F**
56.5	63.8	108	19.3	782	11.1	181	1.49
1395	-	71.3	23.6	617	1.24	-	-
26.3	-	38.3	12.7	1087	2.07	-	-
1695	36.1	17.3	37.5	530	4.02	126	2.68

Table 6: Gas chemistry for pad B wells on January 2015.

Well	mmoles/100 moles steam						
	CO_2	**H_2S**	**NH_3**	**H_2**	**Ar**	**N_2**	**CH_4**
1	1034	63.4	-	-	-	-	-
2	807	41.7	1.32	1.588	0.367	31.131	2.363
3	766	73.6	-	1.423	-	224.30	3.643
4	3892	68	-	3.073	-	245.22	20.70

To compare the relationship of the well fluids to each other, a Cl-SO_4-HCO_3 ternary diagram (Figure 18) and a Na-K-Mg ternary diagram (Figure 19) are given.

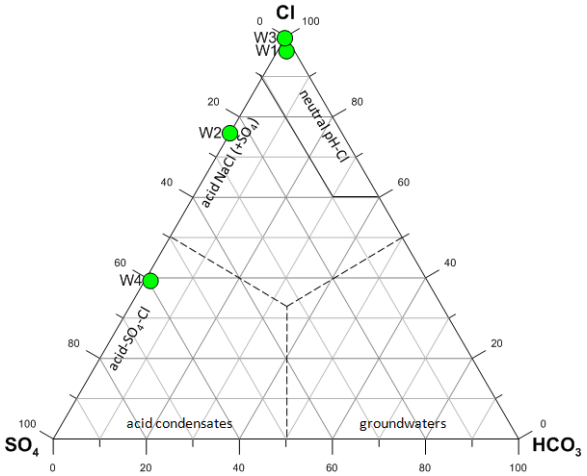

Figure 18: Cl-SO4-HCO3 ternary diagram of pad B wells.

Figure 18 shows the types of fluids produced from each well. Well 1 stays true to its near-neutral pH nature, while near-neutral pH well 4 is located near the acid-SO4 line due to its low HCO_3 and high SO_4 (Table 5). Wells 2 and 3 are both low in pH which explains its lack of HCO_3 (Table 5). This resulted to both wells falling on the acid-NaCl line.

On the other hand, Figure 19 determines the maturity and temperature of the fluid from each well. Well 1 has no Mg data available which may have led to it being categorised as equilibrated water. Wells 2, 3 and 4 are all partially equilibrated since they are situated between the equilibrated water and immature water curves. The produced chemistries of these three wells may change with time as they mature.

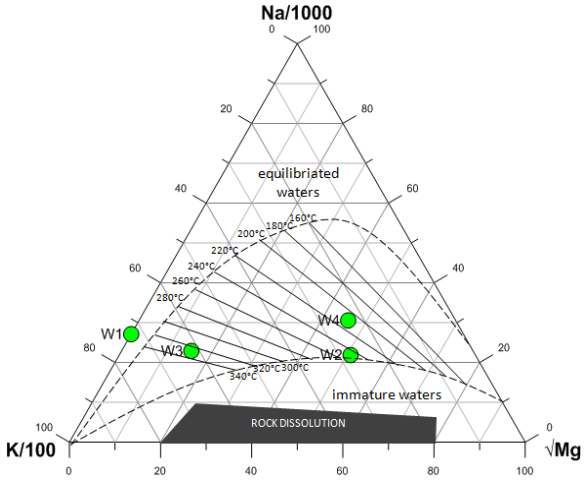

Figure 19: Na-K-Mg ternary diagram of pad B wells.

The temperatures determined from Figure 19 show wells 1 and 3 as the hottest wells (~330°C). Overall, the pad B wells are relatively hot with well 2 at ~250°C and well 4 at ~210°C.

The unusual chemistry of well 3 (low-pH, high-silica) is caused by a deep-seated acidic hydrothermal fluid that taps the bottom or beyond the wellbore. This fluid then passes through biotite-bearing hornblende pyroxene andesite, highly altered andesite-dacite tuff breccias, silicified dacite and andesite breccias, and fresh hornblende andesite lava where its low-pH dissolves some of the rocks which increase the fluid's silica concentration. The other wells were not able to tap into the acidic fluid since the other wells were drilled in the opposite direction of well 3.

4.1 Background on the February 2015 Inspection

We will be focusing on the February 2015 maintenance inspection. Mineral scaling was anticipated during this inspection due to the relatively higher pH and high mass flow rate of the newly introduced well 1.

The maintenance inspection and cleaning was scheduled on February 2015 due to observed increase in scale deposition throughout the system. Separated brine pH was measured and observed to increase from 3.99 (January 6, 2014) to 5.81 (August 20, 2014), which led to more silica scaling. Two-phase header surface temperatures were also declining, which increased the suspicion of massive scaling due to the introduction of well 1. Lastly, the injection well that was accepting the separated brine from Pad B witnessed increase to its well head pressure from vacuum to 0.5 MPag after just two months of utilization.

Two-phase header inspection confirmed the suspected scaling at the mixing point of well 3. As shown in Figure 20A, the header was clear from the end flange until the mixing point of well 3. As suspected, the mixing of the low-pH, high silica well 3 with the near-neutral pH fluids of well 1 resulted in massive scaling at the well 3 mixing point (Figure 20B). Mineral deposits were observed on all sides of the header. Thickness of the scale was 30 cm from the bottom and 13 cm from the top. A sample taken from this area was made of banded magnetite (50%) with sphalerite and hematite, and subrounded fragments (50%) with sphalerite and pyrrhotite (Rosell, et al., 2015).

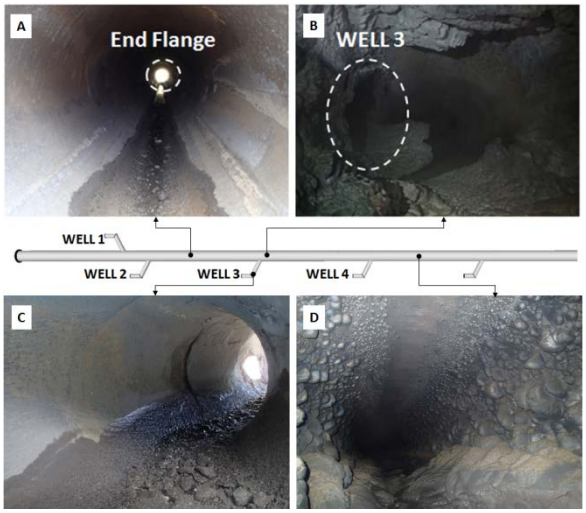

Figure 20: Scaling in pad B two-phase mixing header on February 2015.

Figure 20C shows that the well 3 branch-line before mixing had minimal scaling. Well 3 branch-line scale samples obtained during this inspection were determined to be made of (80%) corrosion products, (10%) amorphous silica and (10%) hematite (Rosell, et al., 2015).

The scaling from the well 3 mixing point continued downstream of well 4 (Figure 20D), and still measured at around 25 cm to 30 cm thick from the bottom of the header. Figure 20D shows silica scale forming globules (protruding structures) of different sizes on the walls. This is not the usual shape of silica scale, which usually forms a jagged surface directed against the fluid flow (Figure 21).

Figure 21: Common silica scaling on a pipe wall.

There is also an observable difference in the scale globule sizes, with the larger formations at the bottom and the smaller globules forming towards the top. Given the large size of the pipe (42" or 106.8 cm) and the two-phase nature of the fluid, it could be concluded that a gas layer formed on the top of the pipe which kept the globules from growing to larger size (Figure 20D).

This mineral scaling declines as the mixed header fluid flows further downstream. At a point approximately 100 m downstream from the end flange, the scale thickness declines to 6 cm and uniformly coats the pipe walls. This further decreases to 2 cm (from the bottom) in another 100 m. The deposits collected from these points were found to be mostly corrosion products made up of magnetite, hematite and pyrrhotite (Rosell, et al., 2015).

4.2 Results and Discussion

Pad B 42" (106.68 cm) two-phase header had a measured pressure of 1.02 MPag. At saturation conditions, this is equivalent to a temperature of 185 °C. The calculated SSI of the individual wells before the inspection is shown in Table 7 below.

Table 7: Silica saturation index of each well in Pad B at 185°C.

Well	Sampling Date	pH	mg/kg		SSI
			SiO_2	Cl	
1	2-Jul-2014	5.49	782	3137	0.9400
2	9-Apr-2014	3.46	617	4398	0.7444
3	30-Jan-2015	3.54	1087	5461	1.316
4	15-Jan-2015	5.59	530	1118	0.6333

Wells 1, 2 and 4 are all undersaturated with respect to silica so mixing them within the two-phase header should pose minimal risk of mineral scaling. However, as shown in Table 7, well 3 is highly supersaturated with silica at an SSI of > 1.3. Determining the saturated silica concentration at the header temperature, well 3 is in excess of 260 mg/kg. Even in the reservoir, well 3 silica concentration is in excess of ~250 mg/kg (Figure 22). This excess silica, however, does not precipitate in the wellbore or the branch-line, due to the low-pH of 3.54.

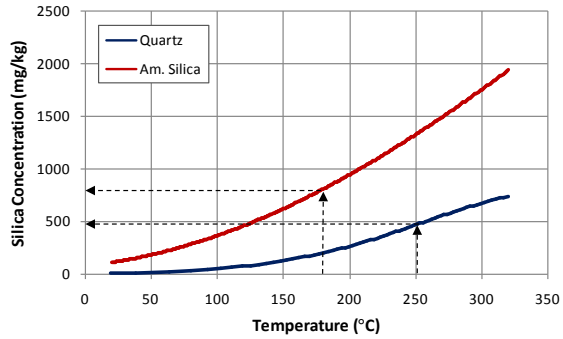

Figure 22: Saturated silica concentration of a fluid at 185°C and 250°C.

The low pH and high silica concentration of well 3 is not related to a sudden change in fluid chemistry. Historically, pH and SiO_2 concentration have been relatively stable since the well was cut into the system in May 2011 (Figure 23).

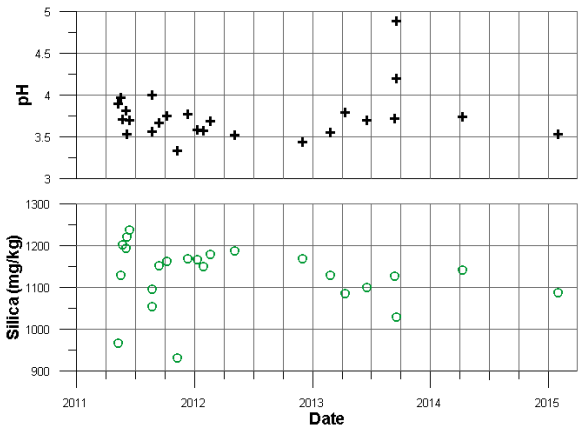

Figure 23: Well 3 historical pH and silica concentration since production started.

When well 3 joined the two-phase header, it mixes with the other well fluids. Table 4 shows that the main contributors to the header, by mass, are wells 1 and 3. When well 1 mixes with the high-silica well 3 fluids, it increases the pH of the fluid to around 5.0. This leads to an instantaneous precipitation of the excess silica and other minerals at the mixing point, as evidenced in the inspection (Figure 20). In effect this is a reversed flashing process common in most steam power plants. For example, the Nga Awa Purua geothermal plant, Addison, et al. (2015) reported acid dosing of the neutral-pH separated brine to reach a pH of 5.0. This keeps the excess ~450 mg/kg silica of the brine, in the solution.

The mineral scales deposited in the 42" (106.68 cm) two-phase header were identified to be made up of mostly silica, iron oxides (magnetite and hematite), iron sulphides (pyrrhotite), and sphalerite. Their corresponding weight percentages from XRD analysis are shown in Figure 24, in relation to the samples location along the header.

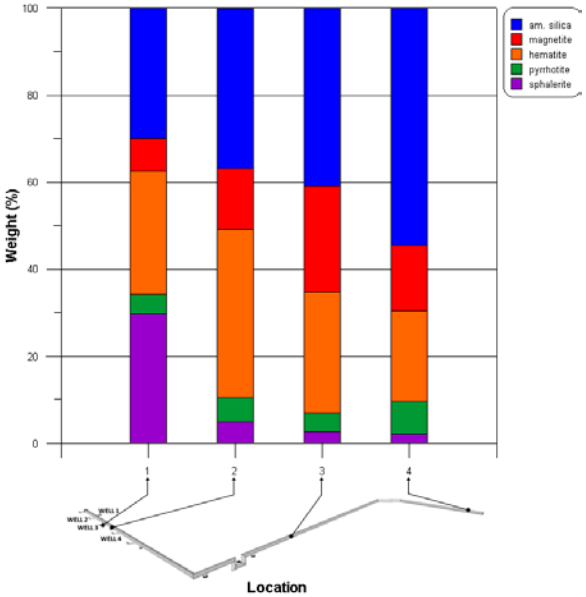

Figure 24: XRD Mineral scale distribution of sample based on its location in pad B two-phase header.

Figure 24 shows sphalerite scales to be more prominent in location 1. Comparing this with the ESEM analysis, the XRD analysis corroborates the presence of overlapping layers of sphalerite and silica in the pipeline. Sphalerite then decreases in sample weight percentage 100 m and 200 m down the pipeline. Zinc was not analysed from the fluid samples; however, there is a significant amount of sulphur from well 2 (Table 5) even if it only contributes a small amount of brine flow (Table 4). The presence of zinc sulphide, combined with the increase in pH, led to the faster precipitation of silica at the well 3 header mixing point.

The iron oxides (magnetite and hematite) and sulphides (pyrrhotite) were consistently present in the XRD analysis (Figure 24); however, they became more prominent in samples 3 and 4 from the ESEM data. With the significant iron content of wells 2 and 3 (Table 5), it is not surprising that these mineral scales would form. The deposition of these minerals takes a longer time to form based on their consistent presence in all the samples and their prominence

in the samples obtained further downstream of the header mixing area.

Figure 24 shows the continuous precipitation of silica throughout the header pipeline. Due to the high silica content of well 3, even the massive silica deposition at the header mixing point (Figure 20B) did not prevent silica scaling further downstream of the header. The scale thickness does decline along the way but the weight percentage of silica still continues to increase (Figure 24). At location 4, silica deposits are still present, but in significantly smaller amounts.

4.3 Recommended Solutions

The cause of the massive scaling at the pad B two-phase header is the mixture of the low-pH, high-silica well 3 fluid with the near-neutral pH fluids of well 1. Based on the SSI of well 3, it is best to handle silica supersaturation before it mixes with the header fluids.

4.3.1 Throttling of Low-pH, High-silica Well 3

Well 3 could be throttled to minimise its flow into the header. This will also minimise the silica supersaturated fluid that mixes with the header fluids. However, this is not ideal since well 3 have a high enthalpy and mass flow rate which will mean a significant generation loss.

4.3.2 Reducing Time between clearing work-over

Frequent shutdown of the system would lead to thinner scale formation along the pipeline. This would enable easier removal of the scales due to the cooling of the pipe which leads to dislodging of the scales from thermal compression. Hydroblasting would also be faster with less deposition to remove. However, this needs to be analysed economically for its effects on the decreased steam production form pad B and the cost of frequent shutdowns.

4.3.3 Installation of Separate Two-Phase Header

The fluid of well 3 could also be separated from the other wells to prevent mineral scaling at the header. Well 2 can be combined with well 3 in a common header, since they have similar pH values and well 2 is undersaturated with respect to silica (Table 7). Wells 1 and 4 will share a separate common header. These two headers will then be directed to different dedicated separator vessels to ensure that their fluids do not mix. However, unless more wells are drilled in pad B in the future, this might not be an economical solution. The construction of a new two-phase header pipeline and a separator vessel dedicated to that pipeline would be costly.

4.3.4 pH Modification of Mixed Header Fluid

Mixing of well 3 with the header fluids causes precipitation of scale due to the sudden increase in pH. Acid dosing could return the pH back to 3.5 and keep the silica suspended in the solution; however, this would lead to corrosion issues along the two-phase pipeline and further downstream. Even if the corrosion issues could be mitigated, the high mass flow inside the header would entail large volumes of acid to be dosed. This would prove to be uneconomical in the long run. Going the other route and increasing the pH to 9.0 by dosing with a base would utilise a larger volume of chemical since it would have to raise the pH from around 5.0. The addition of a base, like caustic soda, will also have other effects and may even promote different type mineral scaling.

4.3.5 Installation of a Well Head Separator

A well head separator could be installed on well 3 to separate the high-silica brine before it mixes with the two-phase header. To cut the cost of constructing a dedicated steam line, the separated steam could be mixed directly with the two-phase header within pad B. However, this may lead to slug flow inside the two-phase header which could cause pipe shaking and damage the pipeline. The separated brine, on the other hand, could be directed to a sump or pond to give the excess silica time to precipitate and deposit. Then, it could be sent further downstream for cold injection. This would eliminate the need to construct a separate brine line from pad B to the separator station.

5. SUMMARY AND FUTURE WORKS

Mineral scaling in two-phase pipelines and headers is rare in the geothermal industry. When it occurs, it is usually due to mixing of incompatible fluids within a common header. This is uncommon since well fluids from the same pad are usually similar in chemistry and steam-water ratio. It is not unheard of, however, to have drastically different well fluids within the same pad, as discussed in the two case studies presented. For both cases, the scales produced are silica and metallic minerals, such as magnetite (Fe_3O_4), pyrrhotite (Fe1-xS), sphalerite (ZnS) and iron-substituted sphalerite (Zn(Fe)S).

Pad A two-phase header scaling is caused by small amounts of highly-mineralised brine, entrained in the steam-dominated well 1 fluid, mixing with the water-dominated fluids of wells 2 and 3. The reaction of the entrained brine with the rest of the header fluids causes massive scaling at the header. The best course of action is to remove the well 1 brine before it mixes with the rest of the fluids. This entails a redesign of the existing drain pot system at the header. Installation of baffles inside the over-sized header will direct brine flowing along the wall to fall to the ODPs. An additional design recommendation is the installation of a spin generator and perforated liner inside the over-sized header to increase brine separation via a BLISS process. A vortex separator may also be installed on the well 1 branch-line to reduce the entrained brine in the well 1 steam before it enters the header. Engineering design optimization is needed to customise the resulting system for efficient brine removal.

The pad B two-phase header scaling, on the other hand, is caused by the mixing of low-pH and high-silica well 3 fluid with the near-neutral pH well 1 fluids. The sudden increase in pH of the well 3 fluids causes instantaneous silica precipitation at the mixing point, which is exacerbated by the presence of metal ions in the solution. Prevention of the mineral scaling can be achieved by separating the well 3 fluids from the rest of the header fluids. This can be achieved in two ways: (a) construction of a separate two-phase pipeline to separate the low-pH wells from the near-neutral pH wells, or (b) installation of a well head separator at well 3 which removes the high-silica brine before it mixes with the other fluids in the header. These methods have to be assessed to determine which would be the most economically viable for continuous production.

Future studies may investigate the use of mineral scale inhibitors at the two-phase header if the recommended engineering solutions do not work. Chemical inhibition could be studied further as a solution to the pad B two-phase header scaling.

ACKNOWLEDGEMENTS

The Authors would like to thank: Heavy Engineering Research Association (HERA) of New Zealand and Energy Development Corporation (EDC) of the Philippines for funding this study.

REFERENCES

Addison, S. J., Winick, J. A., Sewell, S. M., Buscarlet, E., Hernandez, D., & Siega, F. L. (2015). Geochemical Response of the Rotokawa Reservoir to the First 5 Years of Nga Awa Purua Production. New Zealand Geothermal Workshop. Taupo, New Zealand.

Arifien, B. N., Zarrouk, S. J., & Kurniawan, W. (2015). Scrubbing Lines in Geothermal Power Generation Systems. New Zealand Geothermal Workshop. Taupo, New Zealand.

Barbier, E. (2002). Geothermal Energy Technology and Current Status: An Overview. Renewable and Sustainable Energy Reviews , 6 (3-65).

Formento, R. B., & Zarrouk, S. J. (2012). Scaling and Corrosion in Geothermal Development: A Worldwide Review. The University of Auckland, Department of Engineering Science, Auckland.

Gupta, H. K., & Roy, S. (2006). Geothermal Energy: An Alternative Resource for the 21st Century. ProQuest ebrary . Amsterdam, NLD: Elsevier Science & Technology. Retrieved October 12, 2015

Hjartarson, S., Sævarsdóttir, G., Pálsson, H., Ingason, K., Pálsson, B., & Harvey, W. (2012). Utilization of CHloride Bearing, Superheated Steam. Workshop on Geothermal Reservoir Engineering. Standford, California: Standford University.

Jung, D. B., & Wai, K. K. (2000). BLISS: Boundary Layer Inline Separator Scrubber. World Geothermal Congress. Kyushu-Tohoku, Japan: International Geothermal Association.

Lee, K. C. (1995). Performance of a Model In-Line Vortex Separator. World Geothermal Congress. Florence, Italy: International Geothermal Association.

Phillips, S. L., Mathur, A. K., & Garrison, W. (1979). Treatment Methods for Geothermal Brines. In L. A. Caspar, & T. R. Pinchback, Geothermal Scaling and Corrosion (Vol. ASTM Special Technical Publication 717, pp. 207-224). Philadelphia, Pennsylvania: American Society for Testing and Materials.

Ramos, S. G. (2013). Proprietary Internal Report. Energy Development Corporation.

Rosell, J. B., & Concepcion, R. B. (2015). Proprietary Internal Report. Energy Development Corporation.

Scheiber, J., Seibt, A., Birner, J., Genter, A., Cuenot, N., & Moeckes, W. (2015). Scale Inhibition at the Soultz-sous-Forets (France) EGS Site: Laboratory and On-Site Studies. World Geothermal Congress. Melbourne, Australia.

Tassew, M. (2001). Effect of Solid Deposition on Geothermal Utilization and Methods of Control. Geothermal Training Programme. Reykjavik, Iceland: The United Nations University.

van Rosmalen, G. (1983). Scale Prevention with Special Reference to Threshold Treatment. Chemical Engineering Communications , 20:3-4, 209-233.

Villaseñor, L. B., & Calibugan, A. A. (2011). Silica Scaling in Tiwi - Current Solutions. International Workshop on Mineral Scaling. Manila, Philippines.

Zarrouk, S. J., Woodhurst, B. C., & Morris, C. (2014). Silica scaling in geothermal heat exchangers and its impact on pressure drop and performance: Wairakei binary plant, New Zealand. Geothermics, 51, 445-459.